Self-Decoupling of $^{15}N-^{14}N$ Dipole−Quadrupole Couplings in ^{15}N CPMAS NMR Spectra and Molecular Motions in Crystalline Hydrazine Sulfate, *p*-(Diethylamino)benzaldehyde Diphenylhydrazone, and Its Solid Solution in Polycarbonate

Christof-Gottfried Hoelger, Ernst Rössler,[1a] Bernd Wehrle,[1b] Francisco Aguilar-Parrilla, and Hans-Heinrich Limbach*

Institut für Organische Chemie, Takustrasse 3, Freie Universität Berlin, 14195 Berlin, Germany

Received: May 4, 1995; In Final Form: July 19, 1995[⊗]

Self-decoupling of $^{15}N-^{14}N$ dipole−quadrupole couplings was studied by variable temperature ^{15}N CPMAS line-shape analysis of singly ^{15}N-labeled hydrazine sulfate and (diethylamino)benzaldehyde diphenylhydrazone in various solid phases. This phenomenon is caused by molecular motions leading to fast ^{14}N longitudinal relaxation. In the crystalline room temperature phase of hydrazine sulfate, these motions are identified as 180° jumps of hydrazonium perpendicular to the NN-axis. *p*-(Diethylamino)benzaldehyde diphenylhydrazone (DEH) is used as a charge transport agent in organic layered photoconductors. In the crystalline state of this compound, no self-decoupling is observed; in contrast, self-decoupling is observed in solid solutions of DEH in bisphenol A polycarbonate (PC), indicating the presence of molecular motions causing fast ^{14}N longitudinal relaxation. We assign these motions to an internal mobility of the phenyl groups of DEH in the glassy solution. The ^{15}N CPMAS NMR line shapes are interpreted in terms of a broad distribution of activation energies of the motions.

Introduction

It is well-known that the dipolar interaction between spin $S = 1/2$ and $I > 1/2$ nuclei embedded in powdered solids is not totally averaged out by magic angle spinning (MAS). This second-order effect arises due to the fact that the quadrupole interaction of the I-spin is often so large it cannot be treated as a negligible perturbation of the Zeeman interaction.[2-5] As a result, the line positions of S under MAS conditions depend on the spin state of I. In the case where $I = 1$ and the J-coupling is negligible a doublet with a splitting in the range of up to several hundred hertz is observed. The two doublet lines stem from the spin states $m_I = \pm 1$ and $m_I = 0$ showing an intensity ratio of 2:1. Each individual doublet line represents a reduced powder pattern, whose fine structure, however, is rarely resolved.

These splittings facilitate signal assignments, e.g. in ^{13}C CPMAS spectra the assignment of ^{13}C bound to ^{14}N,[2,6] but they can also be a source of information about molecular dynamics. I spin lattice relaxation characterized by the transition rate constant k_t can be very effficient because of the quadrupole moment of I. In this case, fast thermally induced transitions between the spin states occur, influencing the line shape of the 2:1 doublet in the same way as a classical chemical exchange between two powder spectra. As the transition rate constant k_t increases, the lines of the S-spin doublet broaden, coalesce, and become a sharp line at the position of the isotropic chemical shift. This self-decoupling of the dipole−quadrupole splitting was theoretically described by Olivieri[8,9] and Johnson;[10] the behavior can somehow be compared to the case of J-coupled $^1H-^{14}N$ spin pairs in solution. Several authors described examples where the dipole−quadrupole splitting is absent because of complete self-decoupling[7a-c] using a ^{13}C stimulated echo technique, Kennedy et al.[7d] measured slow ^{14}N transition rate constants between 0.04 and 5 s^{-1}.

In this paper we report two examples of $S-I$ dipole−quadrupole self-decoupling, and we show that qualitative and even quantitative information concerning the molecular dynamics can be obtained from the analysis of the variable temperature CPMAS NMR spectra of the S-spins. Actually, we report the results of variable temperature ^{15}N CPMAS NMR studies of different crystalline phases of singly ^{15}N-labeled hydrazine sulfate and of *p*-(diethylamino)benzaldehyde (DEH) in the crystalline state and in glassy solution in bisphenol A polycarbonate (PC). Whereas hydrazine sulfate has also been studied by various methods, only very little information is available on DEH. The interest in DEH stems from the fact that it is employed as a charge carrier for the electron hole transport by thermally activated hopping in organic layered photoconductors. We think that the mobility of charge carrier molecules could be an interesting property for the electron hole conducting process.

Theory

The theory for the calculations of signal patterns of S-spins coupled to quadrupolar I-spin has already been published[3,4,8,18a,25] and will be repeated here only briefly for convenience. The resonance frequency $\nu(m_I)$ of S embedded in a static powder is given by

$$\nu(m_I) = \nu_{zee} - \nu_{cs} - \nu_d(m_I) \quad (1)$$

ν_{zee} is the Larmor frequency, and ν_{cs} describes the chemical shift, as usual. For the dipolar contribution $\nu_d(m_I)$ of a single orientation, Olivieri et al.[4] derived the following equations by first-order perturbation treatment:

[⊗] Abstract published in *Advance ACS Abstracts,* September 1, 1995.

0022-3654/95/2099-14271$09.00/0 © 1995 American Chemical Society

$$\nu_d(m_I = 0) = (3D_{SI}\chi_I/2\nu_I)[\cos\beta_d \cos\theta + \sin\beta_d \sin\theta \cos(\phi-\alpha_d)] \times \{3\cos\theta\cos\beta_d + \eta_q \sin\theta \sin\beta_d \cos(\phi-\alpha_d) - (3\cos^2\theta + \eta_q \sin^2\theta \cos 2\phi) \times [\cos\beta_d \cos\theta + \sin\beta_d \sin\theta \cos(\phi-\alpha_d)]\} \quad (2)$$

$$\nu_d(m_I = \pm 1) = -\nu_d(m_I = 0)/2 \pm D_{SI}(1 - 3[\cos\beta_d \cos\theta + \sin\beta_d \sin\theta \cos(\phi-\alpha_d)]^2) \quad (3)$$

The size of the splitting depends on the dipolar coupling constant D_{SI}, the quadrupole coupling constant χ_I, the Zeeman frequency ν_I, the asymmetry parameter η_I, and the polar angles α_d, β_d of the internuclear vector r_{SI} in the frame of the electric field gradient (EFG) tensor of I; θ and ϕ define the direction of the external magnetic field B_0 in the EFG tensor frame. The equations for ν_{cs} in the EFG tensors frame are given in ref 23. To calculate the MAS average, the EFG tensor is defined in the rotor axis frame by the Euler angles Ψ, Θ, and Φ. Ψ describes the rotation of the sample around the rotor axis, Θ is the angle between the Z-component of the EFG tensor and the rotor axis, and Φ defines the final rotation of the molecule around the Z-component of the EFG tensor. θ and ϕ are then given by

$$\theta = \arccos z \quad (4)$$

$$\phi = \arccos[x/(1-z^2)^{0.5}] \quad (5)$$

where

$$z = -\sin\Theta \cos\Psi \sin\Omega + \cos\Theta \cos\Omega \quad (6)$$

$$x = -\cos\Phi \cos\Theta \cos\Psi \sin\Omega - \cos\Phi \sin\Theta \cos\Omega - \sin\Phi \sin\Psi \sin\Theta \quad (7)$$

Ω is the magic angle between the rotor axis and the direction of the magnetic field. The MAS averaged frequencies $\bar{\nu}(\Omega,\Theta,\Phi,m_I)$ are then obtained by

$$\bar{\nu}(\Omega,\Theta,\Phi,m_I) = {}^1/_2\pi\int_0^{2\pi}\bar{\nu}(\Omega,\Psi,\Theta,\Phi,m_I)\, d\Psi \quad (8)$$

which are numerically calculated for 30 different values of Ψ. The MAS spectrum is then acquired by the addition of 500 different orientations for Θ and Φ and convolution with a line-broadening function. In this study, dynamically broadened spectra were calculated for each orientation in the same way as the classical exchange between two unequally populated sites with frequencies $\bar{\nu}(\Omega,\Theta,\Phi,m_I = 0)$ and $\bar{\nu}(\Omega,\Theta,\Phi,m_I = \pm 1)$ for populations 1 and 2, respectively.[8,18]

Experimental Section

[^{15}N]hydrazine sulfate was synthesized from hydroxylamine-*O*-sulfonic acid and 95% ^{15}N enriched ammonium chloride.[11] The product was recrystallized by evaporation of water from an aqueous solution at 80 °C.

Singly ^{15}N-labeled *p*(diethylamino)benzaldehyde diphenylhydrazone was synthesized in three steps. Firstly, [^{15}N]nitrosodiphenylamine was prepared from diphenylamine and 95% enriched $Na^{15}NO_2$,[12] purchased from Chemotrade Leipzig. [^{15}N]nitrosodiphenylamine was then reduced with Zn/CH_3-COOH to [^{15}N]diphenylhydrazine and isolated as a hydrochloride.[12] In the last step, the hydrazone was prepared by the reaction of saturated solutions of *N,N*-diphenylhydrazine and *p*-(diethylamino)benzaldehyde in ethanol. After 1 h the ethanol was evaporated the residue was treated with water/$CHCl_3$. The organic phase was purified by chromatography on SiO_2/$CHCl_3$. Samples of DEH in PC were prepared by evaporation of appropriate solutions using freshly distilled THF as solvent. The samples were dried in vacuum at 10^{-5} mbar overnight.

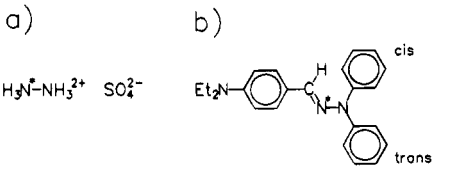

Figure 1. (a) Hydrazine sulfate and (b) *p*-(diethylamino)benzaldehyde diphenylhydrazone (DEH). The asterisk indicates the position of the ^{15}N label.

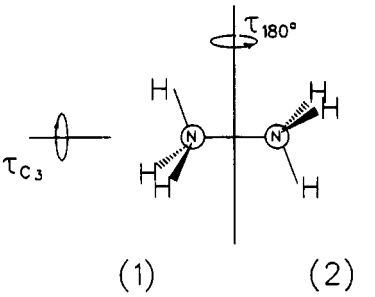

Figure 2. Molecular rotational jumps of $NH_3^+ - NH_3^+$ in hydrazine sulfate.

NMR measurements were performed on a Bruker CXP 100 NMR spectrometer equipped with a 2.1 T superconducting magnet. A 7 mm standard probe head from Doty Scientific Instruments was employed for all measurements. Variable temperature CPMAS NMR was performed using a home-built heat exchanger.[13a] Temperatures were measured by thermoelement places near the rotor and were found to be accurate within ±1 K at the applied spinning speeds.[13b] All spectra are referenced to external solid $^{15}NH_4Cl$.

The Case of [^{15}N]Hydrazine Sulfate

Three modifications of hydrazine sulfate have been found in previous investigations. Room temperature phase B was studied by ^{1}H-T_1, ^{1}H-$T_{1\varrho}$, and ^{2}H NMR and by *x*-ray and neutron diffraction methods.[14-16] The crystal structure shows inequivalent environments for the two nitrogen atoms of the hydrazine molecules, leading to different NH bond length of about 0.03 Å in both $-NH_3^+$ groups. The solid state NMR measurements cited indicate the presence of fast rotational jumps of the $-NH_3^+$ groups around the 3-fold axis (Figure 2). This process is found to be clearly faster in one position than in the other. For the faster process the energy of activation is about 25 kJ/mol. In addition to these dynamics the two nitrogens invert their positions by 180° flips perpendicular to the NN-bond (Figure 2). The Arrhenius parameters of this motion were determined to be approximately $\log(A/s^{-1}) = 12.8$ and $E_a = 40.5$ kJ/mol.[14] At around 220 K, phase B changes to low-temperature phase A, which interconverts only very slowly to phase B at room temperature. In phase A the dynamic behavior was found to be similar for both nitrogens. Additionally, a high-temperature phase C was detected by ^{1}H relaxometry above 480 K. ^{2}H NMR spectra gave evidence of a fast translational diffusion of hydrazine molecules in phase C. ^{14}N NQR measurements were performed at 120 K, showing two sets of NQR parameters;[17] however, it is not clear which phase is concerned.

During the course of our ^{15}N NMR studies of proton transfer in solids we synthesized single ^{15}N-labeled hydrazine sulfate.[18] The ^{15}N CPMAS spectra at 9.12 MHz of this compound between 253 and 348 K are shown in Figure 3. The low-temperature

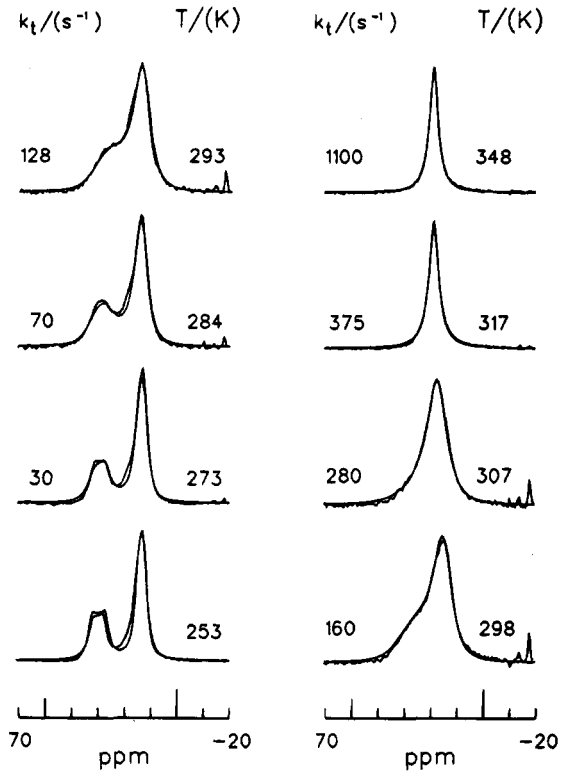

Figure 3. Superposed experimental and calculated ^{15}N CPMAS spectra of [^{15}N]hydrazine sulfate in phase B at 9.12 MHz. For the calculations the following parameters were applied: $\chi = 3.4$ MHz,[12] $\eta_q = 0$; $r_{NN} = 1.44$ Å, $\alpha_d = \beta_d = 0°$.

spectrum at 253 exhibits the typical 2:1 doublet at 19.5 ppm with a splitting of 140 Hz. This spectrum can be well adapted using eqs 1 and 2 and the known parameters. With increasing temperature the lines broaden and coalesce into a single narrow line, which exhibits no change up to 400 K, the highest temperature where spectra were recorded. The high-temperature line exhibits in very good approximation a Lorentzian line shape and appears at the position predicted from the low-temperature spectra and from the spectra of the double-^{15}N-labeled compound. By the analysis shown in Figure 3, the transition rate constants k_t of the ^{14}N-spins were extracted.

The transition rates k_t increase with increasing temperature, indicating that the ^{14}N longitudinal relaxation has not yet passed its minimum value. We assume that the transitions rate constants k_t are linearly related to the rate constant k of a thermally activated process, i.e. that the corresponding ^{14}N longitudinal relaxation is far from its minimum and that eq 9 is valid.

$$k_t = Ck = CA \exp(-E_a/RT) \qquad (9)$$

The Arrhenius curve of the obtained values k_t in Figure 4 is within the margin of error of a straight line, from which we obtain an activation energy of 41.9 ± 2.3 kJ/mol. This value corresponds well with the above mentioned activation energy of 40.5 kJ/mol, which was attributed to the 180° flip motion of hydrazine in phase B. In other words, the ^{14}N-spins are relaxed by 180° flips between two environments exhibiting different EFG tensors. This thesis is corroborated by the following observation. After measurements below 240 K, the room temperature spectrum recorded immediately afterward was found to be similar to the spectrum at 253 K shown in Figure 3. Thus, at low temperature phase A was formed, but at room temperature the conversion from phase A to phase B is hindered; in phase A the ^{14}N transition rates k_t are obviously slow even at a higher

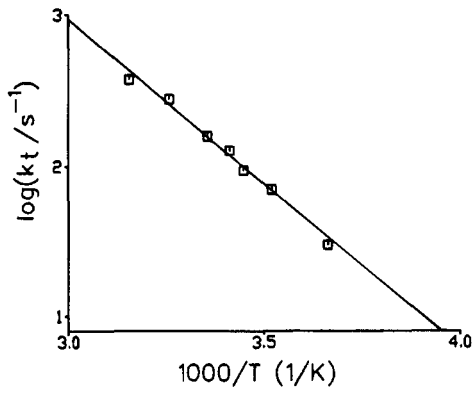

Figure 4. Arrhenius diagram for the transition rates k_t of ^{14}N-spins in phase B of hydrazine sulfate.

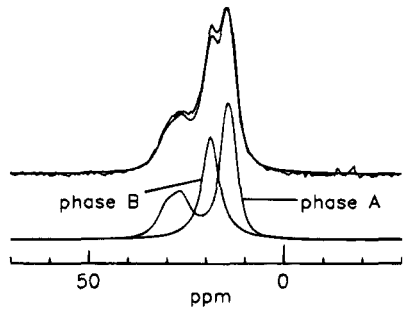

Figure 5. Superposed experimental and calculated ^{15}N CPMAS spectrum of [^{15}N]hydrazine sulfate at 9.12 MHz and 338 K during the slow interconversin from metastable low-temperature phase A to phase B. The contributions of the two phases are shown. The spectrum was calculated using values of $k_t = 48$ s^{-1} for phase A and $k_t = 1000$ s^{-1} for phase B.

temperature. At 338 K the change from phase A to phase B is moderatly fast, leading temporarily to a spectrum with contributions of both phases, as shown in Figure 5. The ^{14}N transition rate k_t in phase A probably remains small at higher temperature, not because the 180° flips are slower in comparison to phase B but because there is no or little change of the ^{14}N EFG tensor due to the higher crystal symmetry. Hydrazine in phase A therefore shows the 2:1 doublet even at higher temperatures, whereas the contribution of phase B at higher temperatures is of a single line. We note that the signal pattern of dipole–quadrupole spin pairs can result from a superposition of signals with differing phases, thus providing information not on the value of the transition rate constant itself but on the amount of molecules with a certain dynamic feature. Such an example is presented in the next section.

The Case of *p*-(diethylamino)benzaldehyde Diphenylhydrazone (DEH)

DEH embedded in polymer matrices is employed as an electron hole transporting agent in organic layered photoconductors.[19-24] Investigations on the structure and the dynamic behavior of medium-sized molecules such as DEH in amorphous environments are still scarce up to date. We decided to synthesize singly ^{15}N-labeled DEH (Figure 1); the ^{15}N label should allow the selective observation of the dye in the polymer matrix without interface from matrix signals.

The ^{15}N CPMAS spectrum of the singly ^{15}N-labeled crystalline DEH depicted in Figure 6a shows the typical 2:1 doublet with a splitting of 150 Hz at 277 ppm. The size of the splitting is within the expected value, but unfortunatly, the quadrupole coupling constant χ_l and the asymmetry parameter η_l in eqs 1 and 2 are unknown, so we were therefore unable to determine the orientation of the ^{14}N EFG tensor with respect to the NN-

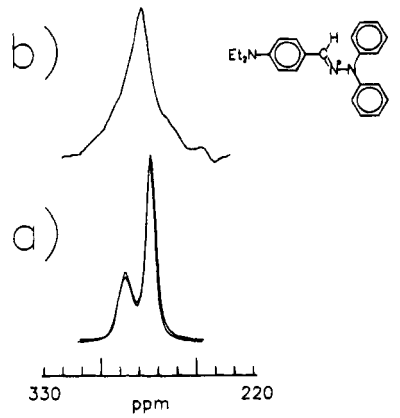

Figure 6. (a) Superposed experimental and calculated room temperature ^{15}N CPMAS spectra of singly ^{15}N-labeled crystalline DEH at 9.12 MHz. The splitting of 150 Hz and the line shapes are compatible with values of $\chi^{14}_N = 3.6-4.6$ MHz, $\eta^{14}_N = 1-0.5$, $\alpha_d = 115-90°$, $\beta = 90°$, $r_{NN} = 1.36$ Å. (b) Room temperature ^{15}N CPMAS spectrum of the amorphous modification.

bond. If DEH is melted and then cooled down, a glassy modification is obtained, which within a few days is slowly interconverted into the crystalline state. The ^{15}N CPMAS spectrum of this glassy modification is shown in Figure 6b. The signal is clearly broadened but shows no signs of asymmetry. We suppose that the splitting is self-decoupled by a dynamic process which leads to fast ^{14}N relaxation; the broadening is probably due to a distribution of isotropic chemical shifts.

Because of improved mechanical properties, DEH is applied in concentrations of up to 40 wt % in polycarbonate films. To avoid complications with remaining crystalline fractions, a solid solution of 15% DEH in PC was prepared and used for this investigation. The ^{15}N CPMAS spectrum of this sample at 303 K (Figure 7) shows a single, low-field-shifted Gaussian-broadened symmetric line at 282 ppm. The spectrum does not change with increasing temperature; when the temperature is decreased, the line slowly changes to the Gaussian-broadened asymmetric doublet at 115 K, again with a splitting of about 150 Hz. In the following we want to discuss this behavior firstly in a qualitative and then in a quantitative way.

Self-decoupling of a dipole−quadrupole splitting of approximately 150 Hz in DEH requires fast ^{14}N relaxation, which for non proton bearing ^{14}N atoms is usually caused by quadrupole relaxation. Effective for the relaxation are motions in the megahertz range, which change the size or the direction of the quadrupole interaction. This motion is suppressed in the crystal but is present in amorphous and probably less rigid environments. The static powder spectra of crystalline DEH and DEH/PC are compared in Figure 8. The main difference between both modifications appears in the presence of the dipolar couplings of ^{15}N to ^{14}N leading to the fine structure in the spectrum of the crystal but which is not resolved in the spectrum of the solid solution. The fact that the observed large anisotropy of the chemical shielding is comparable leads to the conclusion that the imine nitrogen atoms are almost rigid in both modifications. A fast reorientation of the entire diphenylamine unit in both cases is therefore not expected. At room temperature, diphenylamine itself performs fast 180° flips of the phenyl rings, as found by deuterium NMR.[26] The crystal structure of DEH indicates the existence of a large delocalized π-electron system which includes the three nitrogen atoms and the phenyl ring located in the trans-position of the C=N double bond.[19] The rotation of the phenyl ring in the cis-position to the imine carbon atom should be sterically hindered. The ^{14}N relaxation then possibly arises from small changes in the

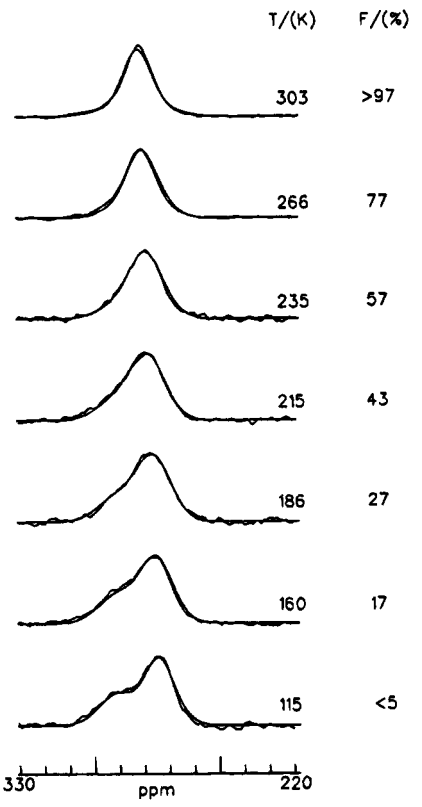

Figure 7. Superposed experimental and calculated ^{15}N CPMAS spectra of 15 wt% DEH in PC at 9.12 MHz. The spectrum at 303 K was fitted as a single Lorentzian line with a half-width of 60 Hz Lorentzian and 40 Hz Gaussian broadening. The low-temperature spectrum at 115 K can be described as an asymmetric 2:1 doublet with parameters obtained from Figure 6 and line width taken from the high-temperature spectrum. The calculated spectra between 160 and 266 K are superpositions of the high-temperature and low-temperature spectra; F is the weight of the high-temperature spectrum. As an alternative, the line shapes can also be described well in terms of a classical dynamic line-shape theory, with transition rate constants k_t at various temperatures being 60 s^{-1}, 160 K; 140 s^{-1}, 186 K; 240 s^{-1}, 215 K; 440 s^{-1}, 235 K; 840 s^{-1}, 266 K. For further discussions see text.

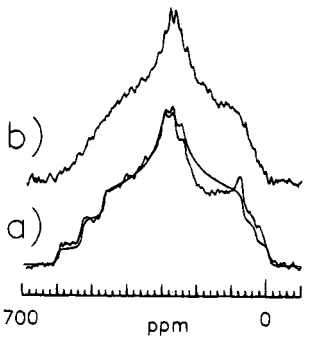

Figure 8. Static ^{15}N powder spectra of DEH at 9.12 MHz at room temperature: (a) DEH crystal, superposed experimental and calculated spectra, dipole and quadrupole parameters as given in Figure 6, $\delta_{11} = 530 \pm 4$ ppm, $\delta_{22} = 268 \pm 4$ ppm, $\delta_{33} = 28 \pm 4$ ppm, $\alpha_{cs} = \alpha_d - \alpha$, $\beta_{cs} = \gamma_{cs} = 0°$. α_{cs}, β_{cs}, and γ_{cs} are Euler angles of the ^{15}N CSA tensor in ^{14}N EFG tensor frame.[25] Polar angles of the NN-vector in the chemical shift principal axis system are $\alpha = 17 \pm 2°$, $\beta = 90 \pm 4°$; β is the angle between δ_{33} and r_{NN}; α is the angle between δ_{11} and the projection of r_{NN} in the δ_{11}/δ_{22} plane. As mentioned in the caption of Figure 6, there is some ambiguity in the evaluation of the quadrupole parameters χ^{14}_N, η_q, and α_d, whereas the value for $\alpha = 17°$ appears valid for all cases. 10 000 scans. (b) DEH in PC, 100 000 scans.

conformation of the diphenylamine unit, which via the delocalized π-system modulates the quadrupole tensor parameters of the amino nitrogen.

The MAS spectra in Figure 7 were simulated by application of the classical line-shape theory, as described above. The obtained transition rates k_t are given in the text of Figure 7. A linear dependence of k_t on the square of temperature, as would be expected for the indirect quadrupole phonon relaxation mechanism,[27] was found. With the assumption of an Arrhenius law (eq 9), we calculated an activation energy of $E_a = 8.5$ kJ/mol. The fact that the transition rates k_t increase with increasing temperature indicates again that the system is still on the low-temperature site of the T_1-minimum. Thus, the rate constant k of the activated process at 300 K must be smaller than 10^7 s^{-1}. The corresponding frequency factor in eq 9 must therefore be smaller than $A = 10^8$ s^{-1}. These values for frequency factor and activation energy are rather small for a unimolecular process which is suppressed in the crystal. This interpretation of the spectra therefore appears unreasonable in our opinion.

An alternative explanation for the data in Figure 7 is given as follows. It is well-known that the dynamics in organic glasses is characterized by broad, temperature-dependent distributions of rate constants and spin lattice relaxation times. Such systems have been described in terms of a temperature-independent distribution for the activation energy.[28] It is interesting to note that for systems such as DEH in PC, which show thermically activated photoconduction, the distribution of energies of electronic states is also an important property for the mobility of charges.[29]

Let us define k_t^* as the ^{14}N transition rate constant causing the coalescence of the ^{15}N dipole−quadrupole splitting. According to eq 9, this corresponds with a rate constant k^*. Assuming a broad distribution of rate constants k, the MAS spectra in Figure 7 can, as in the case of hydrazine, be described in terms of a superposition of two contributions with fractions F and $1 - F$. The first fraction represents the molecules with large transition rates $k_t > k_t^*$ contributing only a single averaged line to the ^{15}N spectra. The second fraction corresponds with molecules possessing small transition rates $k_t < k_t^*$ i.e. contributing a 2:1 doublet to the line shape. The fraction F^* of molecules with $k_t = k_t^*$ is very small. As can be seen in Figure 7, the experimental spectra can be well simulated by the weighted superposition of the spectra at 115 and 303 K. Figure 9 shows a plot of $F\ dF(T)/dT$ versus temperature. As outlined by Rössler et al.,[28] $dF(T)/dT$ is proportional to the fraction F^*, which fulfills the conditions $k = k^*$. This condition is realized at low temperatures for the sites where E_a is small and at high temperatures for sites where E_a is large. In other words, $dF(T)/d(T)$ is a qualitative measure of the temperature-independent distribution of energies of activation $g(E_a)$:

$$dF(T)/dT \sim F^* \sim g(E_a) \qquad (10)$$

The value of E_a can be directly calculated by the corresponding temperature T:

$$E_a = R \ln(k^*/A)T = C^*T,\ k^* = \text{const} \qquad (11)$$

R is the gas constant and A is the frequency factor, as usual. For simplification, k^* and A are assumed to be constant with temperature and the same for all molecules. To estimate C^*, we set $k^* = 10^5-10^6$ s^{-1}—for hydrazine sulfate we obtained $k^* \approx 10^5$ s^{-1}—and A is set to $10^{-13}-10^{12}$ s^{-1}. C^* is then on the order of 154−115 J/(mol K). The function of $F(T)/d(T)$ versus T in Figure 9 exhibits a maximum at around 250 K, which then corresponds according to eq 11 with a value for $E_{a,max} =$ 28−38 kJ/mol and a half-width of the distribution of 15−20 kJ/mol ≅ 0.15−0.19 eV. Details on the shape of the distribution function $g(E_a)$ should not be inferred on the basis of the relatively crude experimental data. It must be emphasized that this interpretation is still tentative, but in contrast to the analysis by application of the classical line-shape theory, as in the case of hydrazine, the value for activation energy $E_{a,max}$ is reasonable and comparable to the values found for 180° phenyl flips in polymers; for example, PC exhibits a value of $E_a = 37$ kJ/mol.[30] The width of the energy of activation distribution function is relatively large but still within the order of magnitude found for the distribution of energies of molecular motions in amorphous organic solids[28] as well as the distribution of energies of electronic state of charge carriers in organic photoconductors, such as triphenylmethane dyes.[29] Effects on the electron hole mobility by polarity of the polymer matrix as well as by the glass transition were measured in organic layered photoconductors.[31] Solid state NMR methods can provide information about structure and mobility of charge carrier molecules, which may lead to a better understanding of such systems on a molecular level.

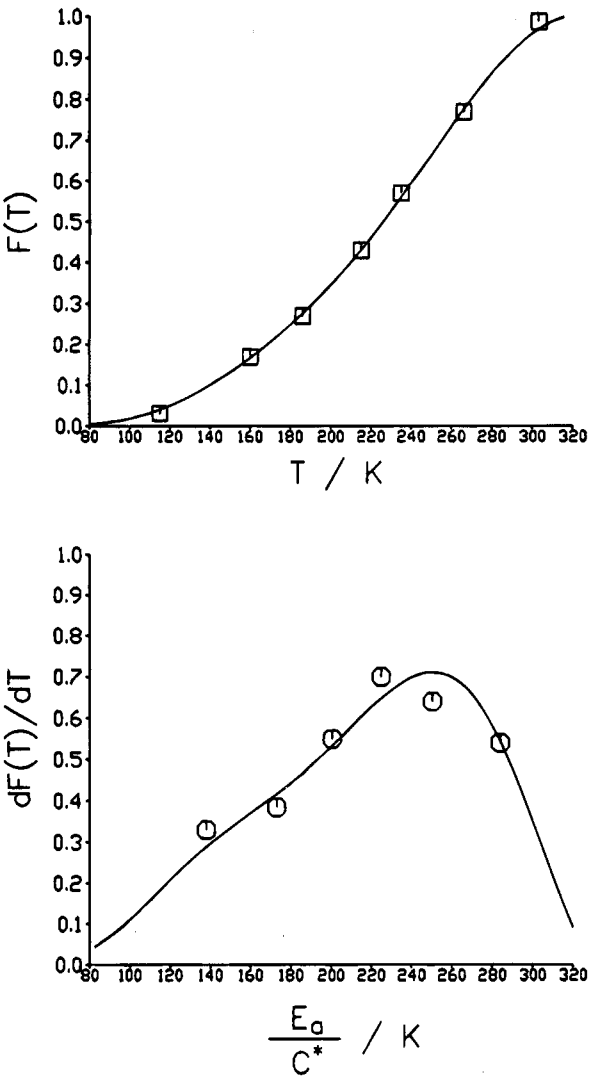

Figure 9. (a) High-temperature fractin $F(T)$ of spectra in Figure 7 versus temperature, experimental points (squares) and fit to a function $F(T) = \exp(aT+b)/(1 + \exp(aT+b))$; $a = 0.0282$ K^{-1}; $b = -6.28$ (solid line). (b) Gradient between experimental points $\Delta F(T)/\Delta T$ (circles) and derivative of fitted curve (solid line).

Conclusions

In the present work we studied the dynamics of two compounds via the temperature-dependent observations of the $^{15}N-^{14}N$ dipole−quadrupole couplings in ^{15}N CPMAS spectra.

In the case of [^{15}N]hydrazine sulfate, the observed behavior is explained by fast 180° jumps of hydrazine, which lead to an exchange of the nitrogens between two different environments in the room temperature phase. This result is in full agreement with the results obtained previously by other methods. The temperature-dependent ^{15}N CPMAS spectra of singly ^{15}N-labeled DEH have been interpreted on the basis of a broad distribution of energies of activation of a motion responsible for the longitudinal relaxation of the ^{14}N nucleus bond to the ^{15}N nucleus monitored. The potential to study dynamics by the line-shape analysis of dipole−quadrupole splittings is relatively low because of the small size of the couplings, especially at higher magnetic fields. On the other hand, in favorable cases interesting additional and qualitative new information on dynamics of a neighboring quadrupole spin can be obtained through the observation of the spin = 1/2 nucleus; for example, a quick check on the presence of a fast molecular motion or of heterogeneity of molecular dynamics in disordered solids is possible.

References and Notes

(1) Present address: Universität Bayreuth, 95440 Bayreuth, FRG. (b) Present address: Bayer AG, 51368 Leverkusen.

(2) Harris, R. K.; Olivieri, A. C. *Prog. Nucl. Magn. Reson. Spectrosc.* **1992**, *24*, 435.

(3) Naito, A.; Ganapathy, S.; McDowell, C. A. *J. Magn. Reson.* **1982**, *48*, 367.

(4) Olivieri, A. C., Frydman, L.; Diaz, L. E. *J. Magn. Reson.* **1987**, *75*, 50.

(5) Hexem, J. G.; Frey, M. H.; Opella, S. J. *J. Chem. Phys.* **1982**, *77*, 3847.

(6) Harris, R. K.; Jonsen, P.; Packer, K. J. *Magn. Reson. Chem.* **1986**, *24*, 977.

(7) (a) Spiess, H. W.; Haeberlen, U.; Zimmermann, H. *J. Magn. Reson.* **1977**, *25*, 55. (b) Power, W. P.; Wasylishen, R. E. *Annu. Rep. NMR Spectrosc.* **1991**, *23*, 60−65. (c) Eichele, K.; Wasylishen, R. E.; Corrigan, J. F.; Doherty, S.; Sun, Y.; Carty, A. J. *Inorg. Chem.* **1993**, *32*, 121. (d) Kennedy, S. D.; Bryant, R. G. *J. Magn. Reson.* **1989**, *83*, 565.

(8) Olivieri, A. C. *J. Magn. Reson.* **1989**, *82*, 342.

(9) Olivieri, A. C. *J. Chem. Soc., Perkin Trans.* **1990**, *2*, 85.

(10) Jonsen, P. *J. Magn. Reson.* **1988**, *77*, 348.

(11) Bak, B.; Christensen, C. H.; Christensen, D.; Hansen, T. S.; Pedersen, E. J.; Nielsen, J. T. *Acta Chem. Scand.* **1965**, *19*, 2434.

(12) Houben Weyl, G. *Methoden der Organischen Chemie*; Thieme Verlag: Stuttgart, New York, 1957; Vol. 10.2, p 226.

(13) (a) Kendrick, R.; Friedrich, S.; Wehrle, B.; Limbach, H.-H.; Yannoni, C. S. *J. Magn. Reson.* **1985**, *65*, 159. (b) Aguilar-Parrilla, F.; Wehrle, B.; Limbach, H.-H.; Bräunling, H *J. Magn. Reson.* **1990**, *87*, 592.

(14) Harrell, J. W.; Peterson, E. M. *J. Chem. Phys.* **1975**, *63*, 3609.

(15) Ratcliffe, C. I. *J. Magn. Reson.* **1980**, *38*, 283.

(16) Power, L. F.; Turner, K. E.; King, J. A. *Acta Crystallogr.* **1975**, *B31*, 2470. Jönson, P.-G.; Hamilton, W. C. *Acta Crystallogr.* **1970**, *B26*, 536.

(17) Grechishkin, V. S.; Anferova, S. V. *Russ. J. Phys. Chem.* **1983**, *57*, 1534.

(18) (a) Hoelger, C.-G.; Limbach, H.-H. *J. Phys. Chem.* **1994**, *98*, 11803. (b) Aguilar-Parrilla, F.; Scherer, G.; Limbach, H.-H.; Foces-Foces, M.; Cano, F. H.; Smith, J. A. S.; Toiron, C.; Elguero, J. *J. Am. Chem. Soc.* **1992**, *114*, 9658. (c) Braun, J.; Schlabach, M.; Wehrle, B.; Köcher, M.; Vogel, E.; Limbach, H.-H. *J. Am. Chem. Soc.* **1994**, *116*, 6593.

(19) Pacansky, J.; Coufal, H. C.; Brown, D. W. *J. Photochem.* **1987**, *37*, 293.

(20) Pacansky, J.; Coufal, H. C.; Waltman, R. J.; Cox, R.; Hsing, C. *Radiat. Phys. Chem.* **1987**, *29*, 219.

(21) Waltman, R. J. Master Degree research report, Department of Materials, Science and Engineering, Stanford University, 1989.

(22) Pacansky, J.; McLean, A. D.; Miller, M. D. *J. Phys. Chem.* **1990**, *94*, 90.

(23) Pai, D. M.; Yanus, J. *Photogr. Sci. Eng.* **1983**, *27*, 14.

(24) (a) Pacansky, J.; Waltman, R.; Grygier, R.; Cox, R. *Chem. Mater.* **1991**, *3*, 454. (b) Pacansky, J.; Waltman, R.; Cox, R. *Chem. Mater.* **1991**, *3*, 903. (c) Pacansky, J.; Waltman, R. *Chem. Mater.* **1991**, *3*, 912.

(25) Curtis, R. D.; Penner, G. H.; Power, W. P.; Wasylishen, R. E. *J. Phys. Chem.* **1990**, *94*, 4000.

(26) Hoelger, C.-G.; Limbach, H.-H. Unpublished.

(27) Abragham, A. *Principles of Nuclear Magnetism*; Oxford University: New York, 1961.

(28) Rössler, E.; Taupitz, M.; Börner, K.; Schulz, M.; Vieth, H.-M. *J. Chem. Phys.* **1990**, *92*, 5847.

(29) Bässler, H. *Phil. Mag. B* **1984**, *50*, 347.

(30) Wehrle, M.; Hellmann, G. P.; Spiess, H. W. *Colloid Polym. Sci.* **1987**, *265*, 815.

(31) (a) Bässler, H.; Schönherr, G.; Abkowitz, M.; Pai, D. M.; *Phys. Rev. B* **1982**, *26*, 3105. (b) Abkowitz, M. A.; McGrane, K. M.; Knier, F. E.; Stolka, M. *Mol. Cryst. Liq. Cryst.* **1990**, *183*, 157.

JP9512568